Acta Acustica 2021, **5**, 37

https://doi.org/10.1051/aacus/2021032

Available online at:
https://acta-acustica.edpsciences.org

TECHNICAL & APPLIED ARTICLE OPEN ACCESS

Microplasma microphones

Philippe Béquin*, Adalbert Nanda Tonlio, and Stéphane Durand

Laboratoire d'Acoustique de l'Université du Mans, UMR CNRS 6613, 72085 Le Mans, France

Received 24 January 2021, Accepted 16 August 2021

Abstract – It is shown experimentally that a microplasma created by a microstructured electrode array is sensitive to sound pressure. In this paper, two electrode architectures are used to create the microplasma. The sensitivity of these microplasma microphones, close to 0.4 nA/Pa, is estimated using a waveguide and a calibration method by comparison with a reference microphone. An empirical expression of the acoustic pressure sensitivity of microdischarges is proposed. The predictions of this empirical model are in good agreement with the experimental data.

Keywords: Microplasma, Electric discharges, Transduction, Microphone, Acoustical measurements and instrumentation

1 Introduction

An ionized gas or plasma is a mixture of electrons, ions and neutrals. In air, at atmospheric pressure, the plasma is generated by applying a DC voltage between two electrodes. In this DC discharge, the current flowing between the electrodes is carried by the free ions and electrons. DC discharges have been intensively studied over the last four decades in the context of medical sterilization, gas cleaning, air pollution control, biological decontamination, material processing, and aerodynamics [1–3]. However, the fine understanding of these discharges is not yet acquired, and there are still many unexplained or poorly modeled phenomena in these intrinsically complex gases.

In acoustics, the desired property is the coupling between a volume of plasma and the surrounding air. More particularly, the interactions between the charged particles and the neutral ones of the plasma and the surrounding gas. The variations in the electric current of the discharge cause pressure fluctuations and the propagation of a sound wave which is the principle of acoustic sources. Conversely, an acoustic wave passing through the plasma volume of a discharge provokes fluctuations in its electrical current which is the principle of acoustic sensors (acoustic pressure and acoustic particle velocity).

Among the acoustic sources using a plasma, the most familiar one is lightning [4]. The spark source is its miniaturized version used mainly in the fields of architectural and urban acoustics for acoustic measurements in scale models [5, 6]. The first acoustic studies on electric arcs began with Du Bois Duddell around the 1900s with the singing arcs [7, 8]. Since then, many acoustic sources using a plasma as an electroacoustic conversion element have emerged. The technical and theoretical developments associated with these sources are given in a review by Bastien in 1987 [9]. Since, other publications came to complete these studies: [10–12] (a non-exhaustive list of references).

In acoustics, the two useful quantities are acoustic pressure and acoustic particle velocity. Though these two quantities should be accessible to measurement by the use of a plasma discharge, there are very few studies considering this kind of measurement. The most recent one is that of Béquin et al. [13] which proposes a plasma velocimeter and an associated electroacoustic model. This work is based on previous studies by Lindvall [14] and Durbin et al. [15] on anemometers. For the measurement of acoustic pressure, only a few plasma microphones have been developed so far [16–23].

The content of this paper completes the experimental work of the same authors on microphonic devices using a plasma as sensing element [16]. In these plasma microphones (Fig. 1), the ionized gas is generated using negative point-to-plane discharges where a DC high negative voltage is applied to the needle electrode placed above a ground plane, metallic electrodes being separated by a millimetric or a sub-millimetric air gap (three-dimensional setup). The microphonic devices studied here use a microplasma array as an electroacoustic conversion element. Two electrodes configurations obtained by microfabrication techniques are used to generate the useful plasma [3, 24]. The electrode gap dimensions in the micrometer range are small enough to generate sufficiently high electric field strengths to ignite discharges by applying only moderate voltages (≃500 V).

*Corresponding author: philippe.bequin@univ-lemans.fr

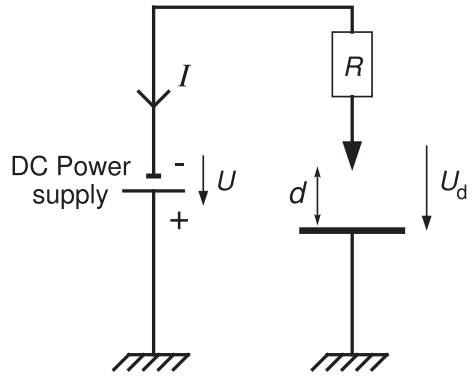

Figure 1. Schematic representation of a negative point-to-plane discharge with metallic electrodes – three-dimensional setup. 100 µm $\leq d \leq$ 3 mm, R = 23 MΩ [16].

2 Microplasma microphone (2D setup)

In the previous paper on microdischarge microphones [16], theoretical and experimental developments are concentrated on individual discharges. Considering now an array of microdischarges arranged in parallel, also called Microstructured Electrode Array, the electrode system can be used as microphone as given in Figure 2. This device consists of plane electrodes bonded to a substrate (two-dimensional setup). More precisely, the two electrodes of 170 points are mounted in parallel and placed facing a wire. The main body is a silica wafer (SiO_2). The electrodes were patterned by photolithography in a chromium-gold layer. A top layer of SiO_2 with a thickness of about 0.5 µm is added to cover these electrodes in order to prevent erosion. In order to stabilize microdischarges, each electrode with points is connected to a ballast resistance ($R \simeq 23$ MΩ).

2.1 Electroacoustic model

The electroacoustic model, which expresses the relation between the variation of the electric current $i(t)$ and the acoustic pressure $p_a(t)$, is given by the semi-empirical relation [16]:

$$S_p = -\frac{i(t)}{p_a(t)} = k\frac{I}{\gamma P_0}\,. \tag{1}$$

The sensitivity S_p is inversely proportional to the ratio of the specific heats $\gamma = \frac{7}{5}$ and the static pressure P_0. It depends on the operating point of the electric discharge (U_d, I) evaluated at P_0. This expression is close to the one proposed by Dayton et al. [19]. The value of the coefficient k is deduced from experimental data. For microdischarges with point-to-plane geometry (Fig. 1), the value of k is close to 1.3. In our case of flat microdischarges obtained with microstructured electrode array, k is set to 1.

3 Experimental work

3.1 DC discharge

A discharge cell is generally composed of two electrodes separated by an air gap d (for example: a point and a plane, see Fig. 1; a multi-point and a wire, see Fig. 2) and a ballast resistance R connected in series. When a DC voltage is applied to the discharge cell, the electric discharge formed between the two electrodes mainly depends on (i) the air pressure, (ii) the applied voltage, (iii) the material of the electrodes, and (iv) the geometry of the discharge [1, 25, 26].

3.2 Voltage current characteristics

The various operating regimes of a DC discharge are determined from the experimental voltage-current characteristic (voltage U_d between the electrodes versus electric current I flowing through the plasma). For point-to-plane discharges (Fig. 1), Figure 3 gives typical examples of voltage-current characteristics. A clear distinction can be observed between millimetric (1 mm $< d <$ 7 mm) and sub-millimetric discharges ($d \leq$ 1 mm). The dynamic behaviors of these discharges are described in the following references: [1, 25, 26].

Figure 4 shows the voltage-current characteristic (U_d, $I = I_r/2$) associated with our microdischarge microphone (Fig. 2). The current I_r collected by the wire electrode is deduced from the voltage drop through a resistance of small value ($r \simeq 50$ Ω). Voltage and current signals are acquired with a voltmeter (type Agilent 34401A) or a fast oscilloscope (type LeCroy LT 322, 500 MHz bandwidth, 200 Ms/s) for DC or time dependent current measurements, respectively.

Due to space-charge effects between the electrodes, the microdischarges have a self-oscillating behavior [27, 28]. The electric current is self-pulsing with a repetition rate of a few tens of kilohertz and pulse durations of the order of a few tens of nanoseconds. It should be noted that array defaults affect the uniform distribution of current between points, ultimately limiting the number of microdischarges that can be created in parallel. With the bombardment of the electrodes by charged particles, the overall shape of the electrodes evolves with time. Microdischarges appear and disappear, and the electric current has a more or less erratic evolution. The particular morphology of this current makes it difficult to estimate its mean value.

The voltage-current characteristic (Fig. 4) displays a negative differential resistance ($R_d = \frac{\Delta U_d}{\Delta I} < 0$), an electrical evolution which is generally associated with the self-oscillating system [29]. The discharge voltage U_d decreases approximately linearly with the mean current I. Its evolution can be modeled using the relation:

$$U_d = U_s + R_d I, \tag{2}$$

where $U_s \simeq 820$ V is the threshold voltage associated with the microdischarge start-up and $R_d \simeq -1.9$ MΩ is the differential resistance. Values of U_s and R_d are deduced from a least squares method. In order to avoid the transition to the spark and stabilize the discharge [24], the Kaufmann criterion must be ensured: $R_d + R > 0$ which is the case with a ballast resistance R close to 23 MΩ.

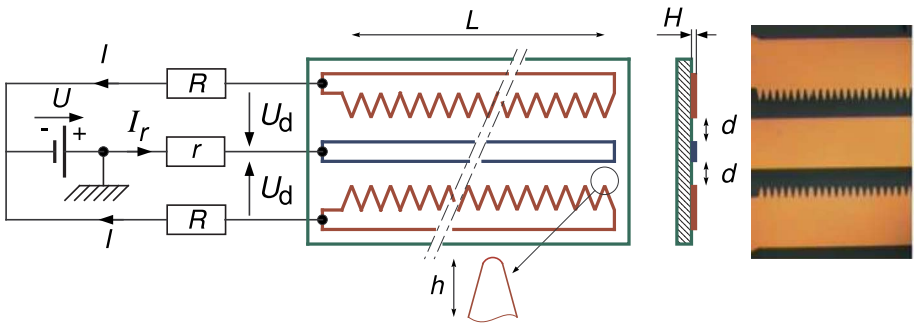

Figure 2. Left side: schematic representation of the microdischarge microphone – two-dimensional setup. Two electrodes with 170 points and a wire electrode. $d = 100$ µm, $L = 17$ mm, $H = 450$ µm, $h = 170$ µm with a tip radius of approximately 20 µm. $R \simeq 23$ MΩ and $r \simeq 50$ Ω are the values of the ballast and shunt resistance. Right side: photograph of a microplasma microphone.

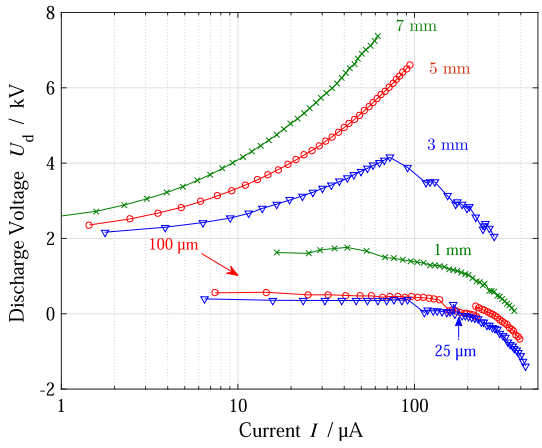

Figure 3. Variation of voltage U_d with mean current I associated with a point-to-plane discharge (Fig. 1) – [16].

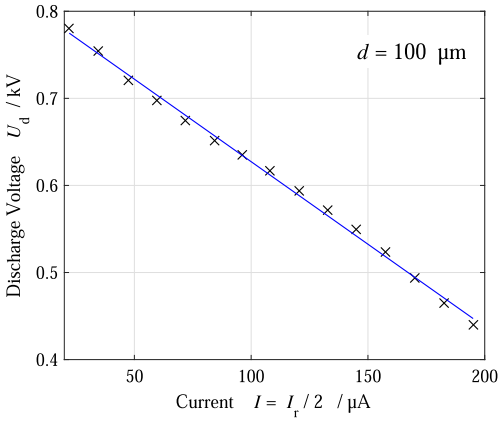

Figure 4. Variation of voltage U_d with mean current I associated with a microstructured electrode array: two electrodes with 170 points and a wire electrode (see Fig. 2). Comparison between experimental data (×××) and empirical model (–), Equation (2), with the adjusted parameters $U_s \simeq 820$ V and $R_d \simeq -1.9$ MΩ deduced from a least squares method.

3.3 Estimating acoustic pressure with a reference microphone and a microplasma microphone

The details and performance of the experimental device used (Fig. 5) are discussed in more details in a previous paper devoted to the plasma microphone [16]. It enables the comparison of the value of the sound pressure deduced from plasma microphone to the one of a reference microphone (using a comparison calibration method). First, acoustic pressure at the center of the tube is measured with a reference microphone (not shown in Fig. 5), the microphone is flush-mounted with the inside wall of the tube. Note that the microplasma microphone is maintained inside the tube in order to take into account its influence on the acoustic field. Then, the acoustic pressure is measured with the microplasma microphone (the reference microphone being removed). As previously described in [16], a computer program is used to drive the frequency, amplitudes, and phases of a dual-channel signal generator (Tektronix AFC – 3022C) which supplies sinusoidal signals to the loudspeakers. A Lock-in Amplifier (SR830 DSP Stanford Research Systems) carries out a synchronous demodulation of its input (voltage from the microphone) by locking its internal oscillator on the phase reference received from the generator (synchronisation output). The measured data are then post-processed by the computer.

Figure 6 shows the sound pressure levels measured in the waveguide with the plasma microphone (with gap length $d = 100$ µm) and the reference microphone for two voltages applied to the loudspeakers ($V_L = 2$ and 3 V_{RMS}). The sensitivity of the plasma microphone is obtained by adjusting its frequency response to that of the reference microphone.

In the frequency range 100–400 Hz, the acoustic device provides an acoustic pressure close to 355 Pa (≃145 dB SPL), which represents a variation in atmospheric pressure P_0 of approximately 0.35%. The plot also reveals peaks in the frequency response (540 Hz, 1.17 kHz, 1.84 kHz, 2.51 kHz, 3.17 kHz, and 3.82 kHz) which are the resonances of the air volume included in the waveguide [16]. Note that the microplasma microphone can measure small pressure

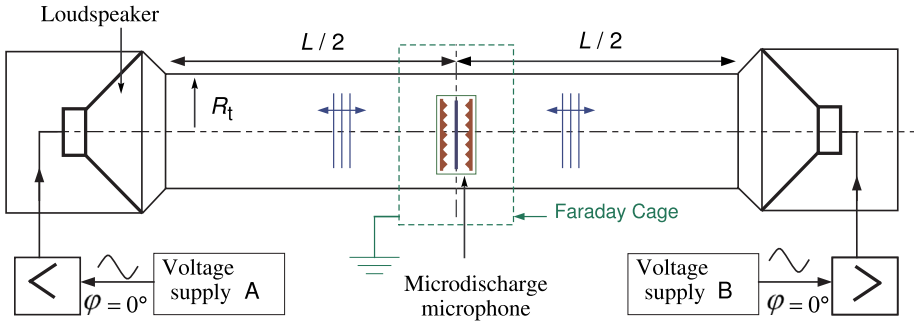

Figure 5. Experimental device used to control the sound pressure at the center of the tube. The sound pressure is first measured with a reference microphone and then with a microplasma microphone. A Faraday cage is placed around a part of the waveguide. $L = 455$ mm and $R_t = 21.9$ mm.

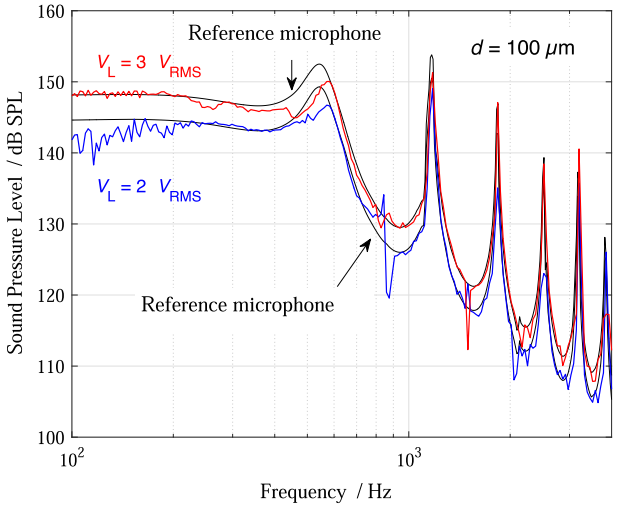

Figure 6. Sound Pressure Level measured with a microplasma microphone ($d = 100$ µm) and a reference microphone for two voltages V_L applied to the loudspeakers. Magnitude in dB SPL: $20 \log(P_{mic}/P_{ref})$ with $P_{ref} = 20 \times 10^{-6}$ Pa. Operating point of the discharge: $U_d \simeq 680$ V, $I \simeq 70$ µA. Fitted sensitivities: $S_{p2V} \simeq 0.46 \times 10^{-9}$ A/Pa and $S_{p3V} \simeq 0.5\ 10^{-6}$ A/Pa.

fluctuations close to 6 Pa (110 dB SPL). The "adjusted" sensitivity of the microplasma microphone is $S_p \approx 0.48 \times 10^{-9}$ A/Pa. Knowing the operating parameters of the microdischarge, the semi-empirical model (Eq. (1)) gives a sensitivity value $S_p = 0.49 \times 10^{-9}$ A/Pa. The predictions of the empirical model are good despite the difficulties in estimating the mean value of the electric current.

The frequency responses in Figure 6 also reveal pressure peaks (with a low amplitude) at frequencies of ≃840 Hz, 1.5 kHz, and 2.2 kHz. As described in reference [16], this is the signature of a sensitivity of the microplasma sensor to the particle velocity. Separating the information on acoustic pressure and particle velocity is therefore necessary. The architecture of the electrodes must be adapted to this function by taking inspiration from anemometry using electric discharges [13–15, 30] for example.

Figure 7 shows the second electrode structure used as microphone. A disk-shaped electrode serves as a single cathode and the anode is a ring-shaped electrode (electrodes without a top layer of SiO_2). A ballast resistor ($R \simeq 23$ MΩ) prevents the transition to the spark. This three-electrode system is designed for particle velocity measurement [13–15, 30]. As in the previous electrode structure (Fig. 1), the electric current is self-oscillating and its erratic character is more pronounced than in the previous electrode system. This fact is mainly due to the absence of a SiO_2 layer on the electrodes. The constant bombardment of the electrodes by charged particles erodes their surface more rapidely and locally changes the inter-electrode distance.

Figure 8 shows the voltage-current characteristic (U_d, I) associated with this electrode structure (Fig. 7). As in the previous case, the discharge voltage U_d decreases approximately linearly with the mean current I ($R_d = \frac{\Delta U_d}{\Delta I} < 0$). Its evolution can be modeled using the relation (2) with $U_s \simeq 595$ V and $R_d \simeq -2.9$ MΩ.

The sensitivity of this microplasma microphone (Fig. 7) is deduced from the experimental setup (waveguide and comparison calibration method) used previously. Figure 9 gives the frequency response of the reference microphone and that of the microplasma microphone (Fig. 7). Its sensitivity is estimated close to 0.4×10^{-9} A/Pa. This frequency response reveals a pressure peak at ≃840 Hz. As in the previous electrode architecture, this sensor also has a sensitivity to the particle velocity. After 2 kHz, Figure 9 shows a significant discrepancy between the frequency responses of the microplasma microphone and the reference microphone. The reason for this difference however is not clear and this tendency must be confirmed by complementary measurements. Knowing the operating parameters of the microdischarge, the empirical model (Eq. (1)) gives a sensitivity value $S_p = 0.42 \times 10^{-9}$ A/Pa. As for the previous case, the predictions of the model are in quite good agreement with the experiment considering the difficulties in estimating the mean value of the electric current. Note that Figure 9 provides a unique frequency response comparison of microphone because the electrode system, as designed, has a limited lifetime, about 15 min compared to 2 h for points systems with a top layer of SiO_2.

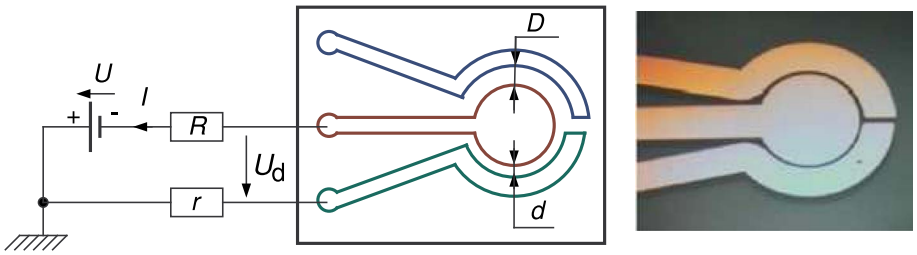

Figure 7. Schematic representation of the microdischarge microphone. The cathode is a disk-shaped electrode. Both anodes are ring-shaped, only one is used. $d = 45$ µm and $D = 60$ µm. $R \simeq 23$ MΩ and $r \simeq 50$ Ω are the values of the ballast and shunt resistance.

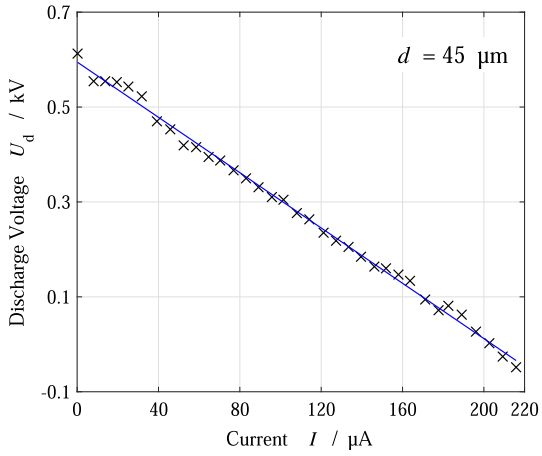

Figure 8. Variation of voltage U_d with current I associated with the microstructured electrode of Figure 7. Comparison between experimental data (×××) and empirical model (–), Equation (2), with the adjusted parameters $U_s \simeq 595$ V and $R_d \simeq -2.9$ MΩ deduced from a least squares method.

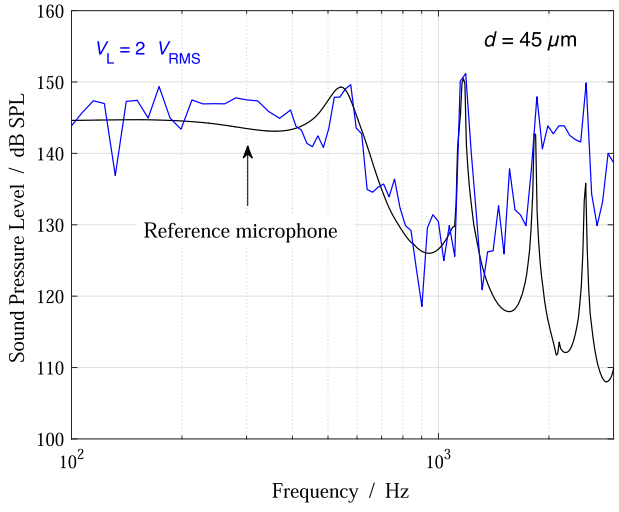

Figure 9. Sound Pressure Level measured with a microdischarge microphone ($d = 45$ µm) and a reference microphone for various voltages V_L applied to the loudspeakers. Magnitude in dB SPL: $20 \log(P_{mic}/P_{ref})$ with $P_{ref} = 20 \times 10^{-6}$ Pa. Operating point of the discharge: $U_d \simeq 420$ V, $I \simeq 60$ µA. Fitted sensitivity: $S_{p2V} \simeq 0.4 \times 10^{-9}$ A/Pa.

4 Summary

This work completes the experimental work of the same authors [16] on the microplasma microphones with point-to-plane geometry. In this paper, we have shown experimentally that a microplasma created by microstructured electrode array is sensitive to sound pressure. The sensitivity of these sensors close to 0.4 nA/Pa is estimated using a waveguide and a calibration method by comparison with a reference microphone. Concerning the electroacoustic sensitivity of these microplasma microphones, the predictions of the proposed empirical model are in good agreement with the experimental data. Unfortunately, the electrode systems as they were manufactured are fragile and their lifetime is limited. This work constitutes a first step in the development of a microplasma microphone. Many theoretical, technical and experimental problems remain to be solved.

Acknowledgments

The authors would like to thank James Blondeau for his assistance in the experiments and his technical advice. Also we would like to thank anonymous reviewers for their valuable comments. This research was funded by the "Région des Pays de la Loire" in the research project MEMSPA (Micro moteurs électrodynamiques pour la réalisation de parois acoustiques absorbantes).

Conflict of interest

Author declared no conflict of interests.

References

1. K.H. Becker, U. Kogelschatz, K.H. Schoenbach, R.J. Barker (Eds.): *Non-equilibrium air plasmas at atmospheric pressure.* Institute of Physics Publishing, London, 2005.
2. P. Bruggeman, R. Brandenburg: Atmospheric pressure discharge filaments and microplasmas: physics, chemistry and diagnostics. *Journal of Physics D: Applied Physics* 46 (2013) 464001.
3. P. Bruggeman, F. Iza, R. Brandenburg: Foundations of atmospheric pressure nonequilibrium plasmas. Plasma Sources Science and Technology 26 (2017) 123002.

4. J.R. Dwyer, M.A. Uman: The physics of lightning. Physics Reports 534 (2014) 147–241.
5. M.F.E. Barron: *Auditorium acoustics and architectural design*. Spun, London, 1993.
6. C. Ayrault, Ph Béquin, S. Baudin: Characteristics of a spark discharge as an adjustable acoustic source for scale model measurements, in: Proceeding of the Acoustics 2012, Nantes, France, 2012.
7. W. Du Bois Duddell: The musical arc. *The Electrician* 52 (1901) 902.
8. J.-M. Ginoux: *History of Nonlinear Oscillations Theory in France (1880–1940)*. Springer, Berlin Heidelberg, 2017.
9. F. Bastien: Acoustics and gas discharges: applications to loudspeakers. *Journal of Physics D: Applied Physics* 20 (1987) 1547–1557.
10. M.S. Mazzola, G.M. Molen: Modeling of a DC glow plasma loudspeaker. Journal of the Acoustical Society of America 81 (1987) 1972–1978.
11. Ph Béquin, K. Castor, Ph Herzog, V. Montembault: Modeling plasma loudspeakers. Journal of the Acoustical Society of America 121 (2007) 1960–1970.
12. Y. Sutton: *Electro-acoustic coupling in a plasma gas.* PhD dissertation, The Open University, Milton Keynes, UK, 2011.
13. Ph Béquin, V. Joly, Ph Herzog: Corona discharge velocimeter. Acta Acustica United With Acustica 104 (2018) 477–485.
14. F.C. Lindvall: A glow discharge anemometer. *IEEE* 53 (1934) 1068–1073.
15. P.A. Durbin, D.J. Mckinzie, E.J. Durbin: An anemometer for highly turbulent or recirculating flows. *Experiments in Fluids* 5 (1987) 184–188.
16. Ph Béquin, A. Nanda Tonlio, S. Durand: Air plasma sensor for the measurement of sound pressure using millimetric and micrometric discharges. Journal of Applied Physics 127 (2020) 034502.
17. P. Thomas: A diaphragmless microphone for radio broadcasting, in: Convention of the AIEE, New York, 1923.
18. I. Dyer, B.W. Blum, U. Ingard: The interaction of a sound wave with a point-to-plane corona discharge. Journal of the Acoustical Society of America 25 (1953) 829–829.
19. J.A. Dayton, J.T. Verdeyen, P.F. Virobik: Method for detecting weak sound waves in a low pressure gas. Review of Scientific Instruments 34 (1963) 1451–1452.
20. W.R. Babcock, R.W. Hermsen: Glow discharge microphone. Review of Scientific Instruments 41 (1970) 1659–1660.
21. F.J. Fransson, E.V. Jansson: The stl-ionophone: transducer properties and construction. Journal of the Acoustical Society of America 58 (1975) 910–915.
22. H. Akino, H. Shimokawa, T. Kikutani, J. Green: On the study of the ionic microphone. Journal of the Audio Engineering Society 62 (2014) 254–264.
23. Ph Béquin, V. Joly, Ph Herzog: Modeling of a corona discharge microphone. *Journal of Physics D: Applied Physics* 46 (2013) 175204.
24. K.H. Schoenbach, K. Becker: 20 years of microplasma research: a status report. European Physical Journal D 70 (2016) 1–22.
25. M. Goldman, A. Goldman: Corona discharges, in: Gaseous Electronics, Hirsh M.N., Oskam H.J., Editors, Academic Press, New York, 1978.
26. Y.P. Raiser: *Gas Discharge Physics*. Springer-Verlag, Berlin Heidelberg, 1991.
27. V.P. Nagorny: Statistical instability of barrier microdischarges operating in townsend regime. Journal of Applied Physics 101 (2007) 023302.
28. C. Lazzaroni, P. Chabert: Discharge resistance and power dissipation in the self-pulsing regime of micro-hollow cathode discharges. Plasma Sources Science and Technology 20 (2011) 055004.
29. A. Jenkins: Self-oscillation. Physics Reports 525 (2013) 167–222.
30. M.D. Yamanaka, H. Hirosawa, Y. Matsuzaka: Glow-discharge ionic anemometer. Review of Scientific Instruments 56 (1985) 617–622.

Cite this article as: Béquin P. Nanda Tonlio A. & Durand S. 2021. Microplasma microphones. Acta Acustica, **5**, 37.